Learning the structure of genetic network dynamics: A geometric approach

Riccardo Porreca [*] **Eugenio Cinquemani** [**] **John Lygeros** [*]
Giancarlo Ferrari-Trecate [***]

[*] *Institut für Automatik, ETH Zürich, Switzerland*
[**] *INRIA Grenoble-Rhône-Alpes, Montbonnot, France*
[***] *Dipartimento di Informatica e Sistemistica, Università di Pavia, Italy*

Abstract: This work concerns the identification of the structure of a genetic network model from measurements of gene product concentrations and synthesis rates. In earlier work, for a wide family of network models, we developed a data preprocessing algorithm that is able to reject many hypotheses on the network structure by testing certain monotonicity properties of the models. Here we develop a geometric analysis of the method. Then, for a relevant subclass of genetic network models, we extend our approach to the combined testing of monotonicity and convexity-like properties associated with the network structures. Theoretical achievements as well as performance of the enhanced methods are illustrated by way of numerical results.

Keywords: Systems Biology, Identification, Quasiconvexity, Unate functions, Sigmoidal activation functions.

1. INTRODUCTION

Genetic networks govern the behavior of living cells in response to changes in the environment, and determine growth, replication, and death of cells. They are composed of genes, i.e. pieces of the DNA strand, that regulate the expression of each other. As a result, protein synthesis is orchestrated by complex biochemical interactions among genes and their products.

Modern technologies for the time-course measurement of gene expression, such as gene reporter systems, allow one to step from pure topological modelling of gene networks to the modelling of the interaction dynamics. However, this requires setting up a dynamical model of the network whose structure and parameters are typically unknown or uncertain. Data-based identification of an accurate model is challenging due to the size of the family of possible model alternatives. Yet, a priori biological knowledge may be exploited so as to ameliorate the complexity of the problem.

In Porreca et al. (2010), we developed an identification strategy for genetic network dynamics with a unate structure. These are ODE models built upon a family of Boolean network models that were argued to capture most of the experimentally observable gene regulation logics (Grefenstette et al., 2006). In particular, we showed that unate models possess *monotonicity properties* that can be tested inexpensively on experimental data, so as to discard entire sets of model hypotheses and focus the search on model structures consistent with the data. One question that arises naturally is whether additional properties of the models in the class can be exploited so as to further narrow down the search for valid models.

In this paper we address this question by considering a subclass of unate models. Leveraging on the observation by Nikolajewa et al. (2007) that most Boolean genetic network models with unate structure belong to an narrower class, called $S_0 \cup S_1$, we show that ODE models with $S_0 \cup S_1$ structure possess *convexity-like properties* that can be used for checking the consistency of different model hypotheses with the experimental data. To this purpose, we introduce a geometric framework that also provides an alternative interpretation of the methods by Porreca et al. (2010). In the economics literature, a similar approach was considered by Hanoch and Rothschild (1972) for testing hypotheses on production processes.

In Section 2 we review our results on the invalidation of unate model structures. In Section 3 we give these results a geometrical interpretation, that we exploit in Section 4 to analyze convexity-like properties of the models with $S_0 \cup S_1$ structure and set up new model invalidation strategies. In Section 5 we discuss possible implementations of these methods. Theoretical and experimental results are discussed in Section 6 by way of illustrative simulations. All mathematical proofs are reported in Appendix A.

2. REVIEW OF RESULTS

We consider ODE models of gene expression of the form (de Jong, 2002)

$$\dot{x}_i = g_i(x) - \gamma_i(x), \tag{1}$$

where $i = 1, \dots, n$ denotes the i-th of n genes, $x_i \geq 0$ denotes the concentration of the corresponding product, $x = (x_1, \dots, x_n)$, and $g_i(x) \geq 0$ and $\gamma_i(x) \geq 0$ are synthesis and degradation rates, respectively. For $i = 1, \dots, n$, we assume that

$$g_i(x) = \kappa_{0,i} + \kappa_{1,i} b_i(x), \tag{2}$$

where $\kappa_{0,i}$ and $\kappa_{1,i}$ are nonnegative constants and $b_i(x)$ is a gene activation level. Typically, $b_i(x)$ is some combination of switch-like regulatory functions (sigmoids) $\sigma^+(x_j)$ or $\sigma^-(x_j) = 1 - \sigma^+(x_j)$, for some $j \in \{1, \dots, n\}$, with possibly unknown parameters θ. Following Porreca et al. (2010), we focus on a particular class of functions $b_i(x)$.

Assumption 1. For some integer $h_i \geq 0$ and some sets of pairwise different indices $J_{il} \subseteq \{1, \dots, n\}$, with $l = 1, \dots, h_i$, let

$$b_i(x) = \prod_{l=1}^{h_i} \left(1 - \prod_{j \in J_{il}} \left(1 - \sigma^{\pm}(x_j)\right)\right), \tag{3}$$

where, for each J_{il} and j, either $\sigma^{\pm}(x_j) = \sigma^+(x_j)$ or $\sigma^{\pm}(x_j) = \sigma^-(x_j)$, with $\sigma^+ : [0, +\infty) \to [0, 1]$ and $\sigma^- : [0, +\infty) \to [0, 1]$ monotone nondecreasing and nonincreasing functions, respectively. By convention, products over an empty set return 1.

In the context of gene expression, (3) is the algebraic counterpart (in the sense of Plahte et al., 1998) of unate Boolean functions, a comprehensive class of gene activation rules where each regulator acts unambiguously either as inhibitor or activator (Grefenstette et al., 2006). By extension, we call (1)–(3) a gene network model with unate structure.

Example 1. A typical choice of sigmoid is the Hill function $\sigma^+(x) = 1/[1 + (\eta/x)^d]$, $x \in \mathbb{R}$. For any choice of the cooperativity parameter $d \geq 1$ and the threshold parameter $\eta \geq 0$, this function increases monotonically from 0 to 1, verifies $\sigma^+(\eta) = 1/2$ and $d\sigma^+(\eta)/d\eta \geq 0$ increases with d. For $d = 1$, in particular, one recovers Michaelis-Menten kinetics. An alternative choice, which we will exploit in this paper, is the logistic function

$$\sigma^+(z) = \frac{1}{1 + e^{-d(z - \tilde{\eta})}}, \qquad z \geq 0, \tag{4}$$

with analogous interpretation for d and $\tilde{\eta}$. Note that in this case $\sigma^+(z) \neq 0$ when $z = 0$. It is immediate to see that Hill functions are in one-to-one correspondence with (4) via the transformations

$$z = \log(x), \quad \tilde{\eta} = \log(\eta). \tag{5}$$

The problem we are concerned with is the invalidation of hypotheses on the structure of (3) (defined by h_i, sets J_{il} and the signs of the sigmoids) on the basis of a dataset $\mathscr{D} = \{(x^k, g_i^k) : k = 1, \dots, m\}$, where each x^k is a vector of protein concentrations and $g_i^k = g_i(x^k)$ is the corresponding synthesis rate. In practice, noisy versions of measurements $\mathscr{D}$ can be obtained by perturbation experiments (see Sontag (2008) and references therein) or time-course experiments (de Jong et al., 2010). For simplicity here we ignore how data are obtained and pretend for the time being that they are noiseless. Presence of noise will be reconsidered in later sections. It is clear that the problem concerns the form of (2)–(3) only. In particular, the specific form of $\gamma_i(x)$ in (1) is irrelevant, as x and g_i are both observed. Since the problem is the same for all genes i, we drop this index from g_i and γ_i. In Porreca et al. (2010) we addressed the problem by exploiting monotonicity properties of $g(x)$. Define the sign pattern $p = (p_1, \dots, p_n) \in \{-1, 0, 1\}^n$ of model (2)–(3) as follows:

$$p_j = \begin{cases} 0, & \text{if } j \notin J_l,\ l = 1, \dots, h, \\ 1, & \text{if } \sigma^{\pm}(x_j) = \sigma^+(x_j), \\ -1, & \text{if } \sigma^{\pm}(x_j) = \sigma^-(x_j). \end{cases}$$

Note that several alternative structures of (3) share the same sign pattern p, e.g. $b(x) = \sigma^+(x_1)\sigma^-(x_2)$ and $b(x) = 1 - (1 - \sigma^+(x_1))(1 - \sigma^-(x_2))$ are both represented by $p = (1, -1)$. Let $g(x|p)$ be any unate model with sign pattern p. In light of Assumption 1, g (and similarly b) is nondecreasing (resp. nonincreasing) in x_j if $p_j = 1$ (resp. if $p_j = -1$), and is independent of x_j if $p_j = 0$.

Proposition 1. For any $l, k \in \{1, \dots, m\}$

$$\Big[p_j(x_j^k - x_j^l) \geq 0,\ j = 1, \dots, n\Big] \Rightarrow \Big[g(x^k|p) - g(x^l|p) \geq 0\Big].$$

Based on this, any model with sign pattern p is invalidated by $\mathscr{D}$ if two indices $l, k \in \{1, \dots, m\}$ exist such that

$$\Big[p_j(x_j^k - x_j^l) \geq 0,\ j = 1, \dots, n\Big] \text{ and } \Big[g^k - g^l < 0\Big]. \tag{6}$$

In this case p is said to be inconsistent (with $\mathscr{D}$).

Remark 1. In Porreca et al. (2010) we further introduced the concept of subpattern, i.e. p' is a subpattern of p if all nonzero entries of p' are equal to the corresponding entries of p. We showed that if p is inconsistent [resp. consistent] then every subpattern [resp. superpattern] p' is also inconsistent [resp. consistent] and used these properties to design an efficient algorithm for the invalidation of entire hierarchies of model structures.

3. A GEOMETRIC APPROACH

For a real-valued function g and $\varepsilon \in \mathbb{R}$, define the super-level set $T_\varepsilon(g) = \{x : g(x) \geq \varepsilon\}$ and the sub-level set $B_\varepsilon(g) = \{x : g(x) \leq \varepsilon\}$. Let $U(p)$ be the family of functions (2) with the unate structure (3) and sign pattern p. We will now show that testing the hypothesis $g \in U(p)$ as in the previous section can be seen as the problem of computing approximations of $T_{g^k}(g)$, with $k \in \{1, \dots, m\}$, from the dataset $\mathscr{D}$. For $x \in \mathbb{R}^n$ and $p \in \{-1, 0, 1\}^n$, define the cone

$$\square(x, p) = \{z \in \mathbb{R}^n : p_j z_j \geq p_j x_j,\ j = 1, \dots, n\}$$

with vertex x (see Fig. 1). Intuitively, for any $g \in U(p)$, p determines the direction of growth of g, hence $\square(x^k, p)$ is a region of $\mathbb{R}^n_{\geq 0}$ where g must be no smaller than g^k.

For $\mathscr{D}' \subseteq \mathscr{D}$, let $\mathcal{K}(\mathscr{D}') \subseteq \{1, \dots, m\}$ be the set of indices of the elements of $\mathscr{D}$ contained in $\mathscr{D}'$ and define

$$M(\mathscr{D}', p) = \bigcup_{k \in \mathcal{K}(\mathscr{D}')} \square(x^k, p), \qquad \mu(\mathscr{D}') = \min_{k \in \mathcal{K}(\mathscr{D}')} g^k.$$

The following result, that is illustrated in Fig. 1, shows that $M(\mathscr{D}', p)$ provides a data-based inner approximation of the set $T_{\mu(\mathscr{D}')}(g)$.

Proposition 2. If $g \in U(p)$ then $M(\mathscr{D}', p) \subseteq T_{\mu(\mathscr{D}')}(g)$.

Based on this property we may redefine inconsistent sign patterns as follows.

Definition 1. A sign pattern p is *m-inconsistent* [1] if there is a (nonempty) set $\mathscr{D}' \subseteq \mathscr{D}$ and $(x^*, g^*) \in \mathscr{D} \setminus \mathscr{D}'$ such that $x^* \in M(\mathscr{D}', p)$ and $g^* < \mu(\mathscr{D}')$. Otherwise p is *m-consistent*.

[1] "m-" stands for monotone.

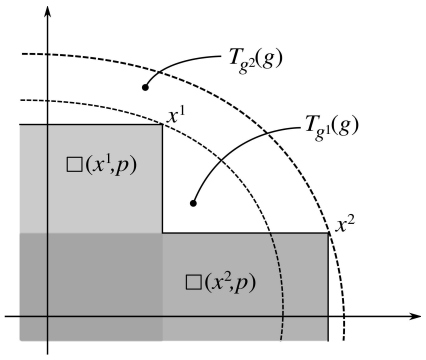

Fig. 1. Cones $\square(x^1, p)$ and $\square(x^2, p)$ composing the set $M(\mathscr{D}')$ for $p = (-1, -1)$, $\mathscr{D} = \{(x^1, g^1), (x^2, g^2)\}$ and $g^2 < g^1$.

It can be checked that Definition 1 is equivalent to the definition of inconsistent sign pattern of Section 2. In particular, the construction of $M(\mathscr{D}', p)$ relies only on the monotonicity properties of g. However, this analysis suggests that any set $M(\mathscr{D}', p)$ such that $M(\mathscr{D}', p) \subseteq T_{\mu(\mathscr{D}')}(g)$ when $g \in U(p)$ can be used to invalidate p by the criterion of Definition 1. The larger the $M(\mathscr{D}', p)$, the higher the chance that points from $\mathscr{D} \setminus \mathscr{D}'$ comply with the requirements of the criterion, i.e. the more models can be invalidated. In the sequel we will investigate how to enlarge $M(\mathscr{D}', p)$ for interesting subclasses of models with unate structure.

4. QUASI-CONVEXITY ANALYSIS OF GENETIC NETWORK MODELS

Let us begin with some basic definitions and results of convex analysis (see Boyd and Vandenberghe (2004) for more details and proofs). Let $D \subseteq \mathbb{R}^n$ be a convex set.

Definition 2. A function $g : D \to \mathbb{R}$ is *quasi-convex* if the following equivalent conditions hold:

i. For every $\alpha \in [0, 1]$ and every $x, y \in D$,
$$g\big(\alpha x + (1-\alpha)y\big) \leq \max\{g(x), g(y)\}; \qquad (7)$$
ii. For every $\varepsilon \in \mathbb{R}$, the sub-level set $B_\varepsilon(g)$ is convex.

g is *quasi-concave* if $-g$ is quasi-convex, i.e.

i'. For every $\alpha \in [0, 1]$ and every $x, y \in D$,
$$f\big(\alpha x + (1-\alpha)y\big) \geq \min\{g(x), g(y)\}; \qquad (8)$$
ii'. For every $\varepsilon \in \mathbb{R}$, the super-level set $T_\varepsilon(g)$ is convex.

Definition 3. A function $g : D \to \mathbb{R}_{>0}$ is *log-convex* if the function $\log(g)$ is convex. Equivalently, for every $\alpha \in [0, 1]$ and every $x, y \in D$,
$$g\big(\alpha x + (1-\alpha)y\big) \leq g(x)^\alpha g(y)^{1-\alpha}.$$
g is *log-concave* if $\log(g)$ is concave, i.e. for every $\alpha \in [0, 1]$ and every $x, y \in D$,
$$g\big(\alpha x + (1-\alpha)y\big) \geq g(x)^\alpha g(y)^{1-\alpha}.$$

Proposition 3. A log-convex (log-concave) function is quasi-convex (quasi-concave).

Log-convexity and log-concavity are easily extended to functions possibly taking the value 0, and the results above still apply.

We now consider two subclasses of unate functions. Recall that $g(x) = \kappa_0 + \kappa_1 b(x)$, with $\kappa_0 \geq 0$ and $\kappa_1 \geq 0$. We say that $g \in S_0$ if
$$b(x) = \sigma^\pm(x_{j_1})\sigma^\pm(x_{j_2})\sigma^\pm(x_{j_3})\sigma^\pm(x_{j_4})\dots\sigma^\pm(x_{j_\ell}) \qquad (9)$$
while $g \in S_1$ if $b(x) = b_\vee(x)b_\wedge(x)$ where
$$b_\vee(x) = \big[1 - \big(1 - \sigma^\pm(x_{j_1})\big)\big(1 - \sigma^\pm(x_{j_2})\big)\big] \qquad (10a)$$
$$b_\wedge(x) = \sigma^\pm(x_{j_3})\sigma^\pm(x_{j_4})\dots\sigma^\pm(x_{j_\ell}) \qquad (10b)$$
for some $\ell \in \{0, \dots, n\}$ and pairwise different indices $j_1, \dots, j_\ell$ from $\{1, \dots, n\}$ [2]. For a given sign pattern p, we will denote the corresponding functions in S_0 and S_1 with $S_0(p)$ and $S_1(p)$. Based on the work by Nikolajewa et al. (2007); Kauffman et al. (2004); Szallasi and Liang (1998), $S_0 \cup S_1$ was proposed in Porreca et al. (2010) as a class of dynamical models describing the majority of the known genetic interaction networks with unate structure.

In the rest of the section we shall make the following hypothesis.

Assumption 2. σ^+ is a logistic function as defined in (4) and $\sigma^- = 1 - \sigma^+$.

Proposition 4. It holds that

a. (9) is log-concave (w.r.t. x and w.r.t. $(x_{j_1} \dots, x_{j_\ell})$) and hence quasi-concave;
b. $b_\vee(x)$ is quasi-convex (w.r.t. (x_{j_1}, x_{j_2})), while $b_\wedge(x)$ is log-concave (w.r.t. $(x_{j_1} \dots, x_{j_\ell})$) and hence quasi-concave.

Note that this result is completely independent of the signs of the sigmoids and the values of the cooperativity and threshold parameters. On the other hand, it can be proven by a counterexample that (10) is generally not log-convex. Note that quasi-convexity is not affected by multiplication by and addition of nonnegative scalars. In practice, this will allow us to infer properties of $b(x)$ from data generated by the function $g(x)$. We now apply these results to the invalidation of models with structure (9) (Section 4.1) and (10) (Section 4.2), under the standing Assumption 2. While Proposition 4 does not hold in general if σ^+ is not the logistic function, the methods derived below also apply to models where σ^+ is a Hill function, up to a log-transformation of data and thresholds (see Section 2).

4.1 Invalidation of models in S_0

For any $\mathscr{D}' \subseteq \mathscr{D}$ and any sign pattern p let $C(\mathscr{D}', p)$ denote the convex hull of all points of $M(\mathscr{D}', p)$. The following result, that is illustrated in Fig. 2, shows that $C(\mathscr{D}', p)$ provides a data-based inner approximation of the set $T_{\mu(\mathscr{D}')}(g)$.

Proposition 5. If $g \in S_0(p)$, then $C(\mathscr{D}', p) \subseteq T_{\mu(\mathscr{D}')}(g)$.

Definition 4. For $g \in S_0$, a sign pattern p is *c-inconsistent* [3] if there is a (nonempty) set $\mathscr{D}' \subseteq \mathscr{D}$ and $(x^*, g^*) \in \mathscr{D} \setminus \mathscr{D}'$ such that $x^* \in C(\mathscr{D}', p)$ and $g^* < \mu(\mathscr{D}')$. Otherwise p is *c-consistent*.

This is an extension of Definition 1 for models in S_0. Since $C(\mathscr{D}', p) \supseteq M(\mathscr{D}', p)$, Definition 4 allows one to invalidate more models.

[2] The notation $b_\vee$ and $b_\wedge$ comes from the fact that (10a) and (10b) may be interpreted as the algebraic counterparts of logical conjunction ($\vee$) and disjunction ($\wedge$), respectively (Porreca et al., 2010).
[3] "c-" stand for convex.

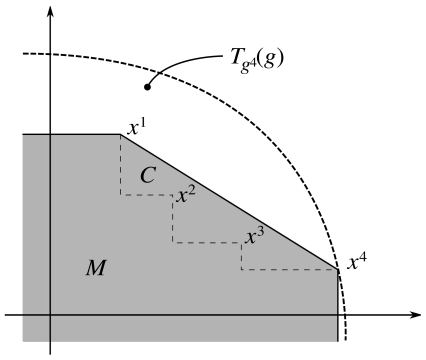

Fig. 2. Sets $C(\mathscr{D}', p)$ (whole gray area) and $M(\mathscr{D}', p)$ for $p = (-1, -1)$, $\mathscr{D} = \{(x^i, g^i), i = 1, \dots, 4\}$ and $g^4 < g^3 < g^2 < g^1$.

4.2 Invalidation of models in S_1

For $g \in S_1$ a convexity-like property does not globally hold. Hence the goal is to combine the different properties of (10a) and of (10b). There are different ways to do so, each leading to different conditions for the invalidation of model structures. We will need the following lemma.

Lemma 6. For $k = 1, \dots, m$ let $a_k \in \mathbb{R}_{\geq 0}$ and $b_k \in \mathbb{R}_{\geq 0}$. Then

$$\min_k a_k b_k \leq \max_k a_k \cdot \min_k b_k \leq \max_k a_k b_k.$$

For a generic $z \in \mathbb{R}^d$ and $p \in \{-1, 0, 1\}^d$, define the cones

$$\square^+(z, p) = \{z' \in \mathbb{R}^d : \ p_j z'_j \geq p_j z_j, \ \forall j = 1, \dots, d\} \ , \tag{11a}$$

$$\square^-(z, p) = \{z' \in \mathbb{R}^d : \ p_j z'_j \leq p_j z_j, \ \forall j = 1, \dots, d\} \ . \tag{11b}$$

Let $j_\vee = \{j_1, j_2\}$ and $j_\wedge = \{j_3, \dots, j_\ell\}$ be the indices of the entries of (10a) and (10b). Let $p_\vee = (p_{j_1}, p_{j_2})$ and $p_\wedge = (p_{j_3}, \dots, p_{j_\ell})$ denote the entries $j_\vee$ and $j_\wedge$ of the sign pattern p. Note that the triplet $(j_\vee, j_\wedge, p)$ defines the structure of (10). For any vector $x \in \mathbb{R}^n_{\geq 0}$ let $x_\vee = (x_{j_1}, x_{j_2})$ and $x_\wedge = (x_{j_3}, \dots, x_{j_\ell})$. Let $b_\vee(x_\vee)$ denote (10a) and $b_\wedge(x_\wedge)$ denote (10b). For any $\mathscr{D}' \subseteq \mathscr{D}$, define the sets

$$L_{\max,\vee}(\mathscr{D}', p_\vee) = \text{Conv}\left(\bigcup_{k \in \mathcal{K}(\mathscr{D}')} \square^-(x^k_\vee, p_\vee)\right), \tag{12a}$$

$$U_{\max,\vee}(\mathscr{D}', p_\vee) = \bigcap_{k \in \mathcal{K}(\mathscr{D}')} \square^+(x^k_\vee, p_\vee), \tag{12b}$$

$$L_{\min,\wedge}(\mathscr{D}', p_\wedge) = \bigcap_{k \in \mathcal{K}(\mathscr{D}')} \square^-(x^k_\wedge, p_\wedge), \tag{12c}$$

$$U_{\min,\wedge}(\mathscr{D}', p_\wedge) = \text{Conv}\left(\bigcup_{k \in \mathcal{K}(\mathscr{D}')} \square^+(x^k_\wedge, p_\wedge)\right), \tag{12d}$$

where Conv denotes convex hull. The next proposition clarifies the approximation properties of sets L and U in (12).

Proposition 7. Let $\mathscr{M}_\vee(\mathscr{D}') = \max\{b_\vee(x^k_\vee) : \ k \in \mathcal{K}(\mathscr{D}')\}$ and $\mu_\wedge(\mathscr{D}') = \min\{b_\wedge(x^k_\wedge) : \ k \in \mathcal{K}(\mathscr{D}')\}$. Then the following implications hold

$$x_\vee \in L_{\max,\vee}(\mathscr{D}', p_\vee) \implies b_\vee(x_\vee) \leq \mathscr{M}_\vee(\mathscr{D}'), \tag{13a}$$

$$x_\vee \in U_{\max,\vee}(\mathscr{D}', p_\vee) \implies b_\vee(x_\vee) \geq \mathscr{M}_\vee(\mathscr{D}'), \tag{13b}$$

$$x_\wedge \in L_{\min,\wedge}(\mathscr{D}', p_\wedge) \implies b_\wedge(x_\wedge) \leq \mu_\wedge(\mathscr{D}'), \tag{13c}$$

$$x_\wedge \in U_{\min,\wedge}(\mathscr{D}', p_\wedge) \implies b_\wedge(x_\wedge) \geq \mu_\wedge(\mathscr{D}'), \tag{13d}$$

Equivalently, one has

$$L_{\max,\vee}(\mathscr{D}', p_\vee) \subseteq B_{\mathscr{M}_\vee(\mathscr{D}')}(b_\vee),$$
$$U_{\max,\vee}(\mathscr{D}', p_\vee) \subseteq T_{\mathscr{M}_\vee(\mathscr{D}')}(b_\vee),$$
$$L_{\min,\wedge}(\mathscr{D}', p_\wedge) \subseteq B_{\mu_\wedge(\mathscr{D}')}(b_\wedge),$$
$$U_{\min,\wedge}(\mathscr{D}', p_\wedge) \subseteq T_{\mu_\wedge(\mathscr{D}')}(b_\wedge).$$

According to (13), points in the various sets U and L provide upperbounds and lowerbounds to minima and maxima of $b_\vee$ and $b_\wedge$ over $\mathscr{D}'$.[4] Equivalently, sets U and L provide inner approximations for the various sets T and B. The idea is now to combine Lemma 6 and Proposition 7 to establish inequalities for $b_\vee(x_\vee) \cdot b_\wedge(x_\wedge)$, and hence for the measured values of $g(x) = \kappa_0 + \kappa_1 b_\vee(x_\vee) \cdot b_\wedge(x_\wedge)$. Recall that $\mu(\mathscr{D}') = \min\{g^k : \ k \in \mathcal{K}(\mathscr{D}')\}$ and let $\mathscr{M}(\mathscr{D}') = \max\{g^k : \ k \in \mathcal{K}(\mathscr{D}')\}$.

Proposition 8. For any (nonempty) set $\mathscr{D}' \subseteq \mathscr{D}$ and $(x^*, g^*) \in \mathscr{D} \setminus \mathscr{D}'$, the following implications hold:

$$\left.\begin{array}{l} x^*_\vee \in L_{\max,\vee}(\mathscr{D}', p_\vee) \\ x^*_\wedge \in L_{\min,\wedge}(\mathscr{D}', p_\wedge) \end{array}\right\} \implies g^* \leq \mathscr{M}(\mathscr{D}'),$$

$$\left.\begin{array}{l} x^*_\vee \in U_{\max,\vee}(\mathscr{D}', p_\vee) \\ x^*_\wedge \in U_{\min,\wedge}(\mathscr{D}', p_\wedge) \end{array}\right\} \implies g^* \geq \mu(\mathscr{D}').$$

From Proposition 8 we may now introduce the following criterion for the invalidation of models in S_1.

Definition 5. For $g \in S_1$, the structure $(j_\vee, j_\wedge, p)$ is *c-inconsistent* if there exists a (nonempty) set $\mathscr{D}'$ and a data point $(x^*, g^*) \in \mathscr{D} \setminus \mathscr{D}'$ such that either of the following conditions applies:

(I) $x^*_\vee \in L_{\max,\vee}(\mathscr{D}', p_\vee)$, $x^*_\wedge \in L_{\min,\wedge}(\mathscr{D}', p_\wedge)$, $g^* > \mathscr{M}(\mathscr{D}')$

(II) $x^*_\vee \in U_{\max,\vee}(\mathscr{D}', p_\vee)$, $x^*_\wedge \in U_{\min,\wedge}(\mathscr{D}', p_\wedge)$, $g^* < \mu(\mathscr{D}')$

The structure $(j_\vee, j_\wedge, p)$ is *c-consistent* if it is not c-inconsistent.

Definition 5, that is illustrated in Fig. 3, is similar to Definition 1 for models in S_1. In particular, when $|\mathscr{D}'| = 1$, condition (II) is equivalent to the condition in Definition 1. Moreover, one can notice that m-inconsistency can be tested by considering singleton sets $|\mathscr{D}'|$ only (see Proposition 1). This means that Definition 5 is an extension of Definition 1 for models in S_1, thus allowing the invalidation of a superset of all m-inconsistent strucures.

Remark 2. Following on Remark 1, for models in both S_0 and S_1, it is possible to establish hierarchical relationships among the *model structures* invalidated by the data. Loosely speaking, one can see that invalidation of a single structure automatically invalidates all model structures obtained by setting to zero certain nonzero entries of p. Note that invalidating hierarchies of model structures does not invalidate all corresponding sign patterns (i.e. alternative structures with the same sign pattern may still be

[4] For example, from (13a) one has that $b_\vee(x_\vee)$ is a lower bound to the max of values $b_\vee(x^k)$ and hence the notation $L_{\max,\vee}$.

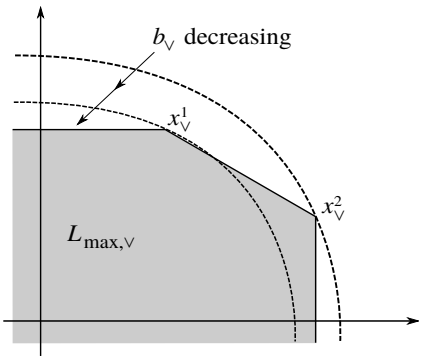

(a) Set $L_{\max,\vee}(\mathscr{D}', p_\vee)$ in the $x_\vee$-plane.

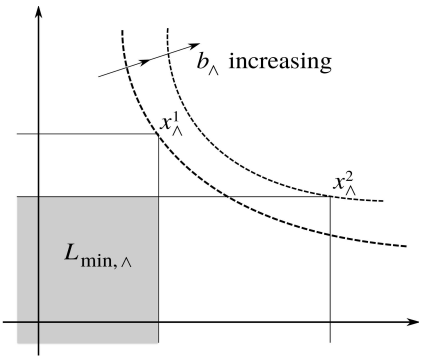

(b) Set $L_{\min,\wedge}(\mathscr{D}', p_\wedge)$ in the $x_\wedge$-plane.

Fig. 3. Sets in condition (I) of Definition 5 for $x \in \mathbb{R}^4$, $\mathscr{D}' = \{x^1, x^2\}$ and $p_\vee = p_\wedge = (1, 1)$.

consistent with the data). This property will be analyzed and exploited more thoroughly in a later work.

5. ALGORITHMS AND IMPLEMENTATION

An efficient method for testing m-inconsistency was proposed in Porreca et al. (2010). The procedure is based on Proposition 1 and hierarchical properties of sign patterns (see Remark 1) rather than on the geometric approach discussed in Section 3. Here we are concerned with the practical use of Definitions 4–5 for testing c-inconsistency of models in $S_0 \cup S_1$. In the following discussion, we will focus on the more complex case of testing S_1 structures and then show how the falsification of S_0 structures can be seen as a particular case of Definition 5-(II).

Our approach to test c-inconsistency is to check if, for any $(x^*, g^*) \in \mathscr{D}$, there exists a set $\mathscr{D}' \subseteq \mathscr{D} \setminus \{(x^*, g^*)\}$ which fulfills either condition (I) or (II) of Definition 5. Focusing on condition (I), it is easily seen that any point (x', g') in $\mathscr{D}'$ must verify

$$[g' < g^*] \quad \text{and} \quad [\mathrm{diag}(p_\wedge)(x'_\wedge - x^*_\wedge) \geq 0] \qquad (14)$$

in order to ensure $g^* > \mathscr{M}(\mathscr{D}')$ and $x^*_\wedge \in L_{\min,\wedge}(\mathscr{D}', p_\wedge)$. Then, one has to check whether $x^*_\vee \in L_{\max,\vee}(\mathscr{D}', p_\vee)$ for the set

$$\mathscr{D}' = \{(x', g') \in \mathscr{D} \setminus \{(x^*, g^*)\} \text{ verifying (14)}\}$$

only.[5] Similarly, in order to fulfill condition (II), $\mathscr{D}'$ is constructed as the set of points verifying

$$[g' > g^*] \quad \text{and} \quad [\mathrm{diag}(p_\vee)(x'_\vee - x^*_\vee) \leq 0] \ . \qquad (15)$$

[5] This follows from the property that $L_{\min,\wedge}(\mathscr{D}'', p_\wedge) \subseteq L_{\min,\wedge}(\mathscr{D}', p_\wedge)$ for any $\mathscr{D}'' \subseteq \mathscr{D}'$.

Algorithm 1. c-inconsistency test for a structure $(j_\vee, j_\wedge, p)$

1: **for** all $(x^*, g^*) \in \mathscr{D}$ **do**
2: $\quad \mathscr{D}' = \{(x', g') \in \mathscr{D} \setminus \{(x^*, g^*)\}$ verifying (14)$\}$
3: $\quad$ **if** $x^*_\vee \in L_{\max,\vee}(\mathscr{D}', p_\vee)$ **then**
4: $\quad\quad$ label $(j_\vee, j_\wedge, p)$ as c-inconsistent and exit
5: $\quad$ **end if**
6: $\quad \mathscr{D}' = \{(x', g') \in \mathscr{D} \setminus \{(x^*, g^*)\}$ verifying (15)$\}$
7: $\quad$ **if** $x^*_\wedge \in U_{\min,\wedge}(\mathscr{D}', p_\wedge)$ **then**
8: $\quad\quad$ label $(j_\vee, j_\wedge, p)$ as c-inconsistent and exit
9: $\quad$ **end if**
10: **end for**
11: label $(j_\vee, j_\wedge, p)$ as c-consistent

The complete method for testing c-inconsistency of a given structure is summarized in Algorithm 1.

Since $C(\mathscr{D}', p) = U_{\min,\wedge}(\mathscr{D}', p)$, condition (II) in Definition 5 is also a valid test for S_0 structures, where $x_\vee$ and $p_\vee$ are empty. In this case, condition (I) is not of interest hence one can ignore lines 2–5 in Algorithm 1.

As already mentioned, Definitions 4–5 provide extensions of m-inconsistency, meaning that all structures $(j_\vee, j_\wedge, p)$ associated with an m-inconsistent pattern p are also c-inconsistent. However, Algorithm 1 involves the construction of convex hulls, making c-inconsistency tests more computationally demanding than m-inconsistency tests, for which the efficient algorithm in Porreca et al. (2010) can be applied. Therefore, substantial computational savings can be achieved using the following procedure:

- assess m-inconsistency of sign patterns by means of the algorithm in Porreca et al. (2010);
- for all m-inconsistent patterns p, label all structures $(j_\vee, j_\wedge, p)$ as inconsistent;
- for all m-consistent patterns p, test consistency of any structure $(j_\vee, j_\wedge, p)$ using Algorithm 1.

The combined procedure was implemented in Matlab 7.10 (R2010a), resorting to the Multi-Parametric Toolbox (MPT, Kvasnica et al., 2004) for the computation of convex hulls.

5.1 Handling noisy data

To deal with noisy measurements of (x^k, g^k) in $\mathscr{D}$, we follow a *robust* approach. We assume lower and upper bounds $l(\cdot)$ and $u(\cdot)$ to be available for the true values of g^k and x^k_j, $j = 1, \ldots, n$. This means that every x^k is surrounded by an uncertainty box. In practice, the example in the next section shows that this approach is still viable in the case of Gaussian (unbounded) noise affecting the data.

The idea is to robustify all inconsistency conditions by taking the bounded uncertainty into account. While this is trivial for conditions on data g^k, robustification is easily achieved also for all tests involving data x^k. As an example, condition $x^*_\vee \in L_{\max,\vee}(\mathscr{D}', p_\vee)$ for $p_\vee = (1, 1)$ is robustified by considering the worst-case inner approximation of $L_{\max,\vee}(\mathscr{D}', p_\vee)$, i.e. by testing whether $(u(x^*_{j_1}), u(x^*_{j_2}))$ belongs to the set

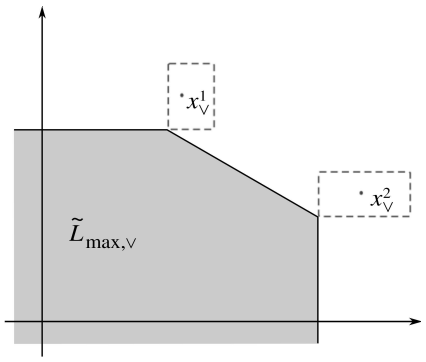

Fig. 4. Uncertainty boxes (dashed) and the set $\tilde{L}_{\max,\vee}(\mathscr{D}', p_\vee)$ in (16) for $\mathscr{D}' = \{x^1, x^2\}$ and $p_\vee = (1, 1)$.

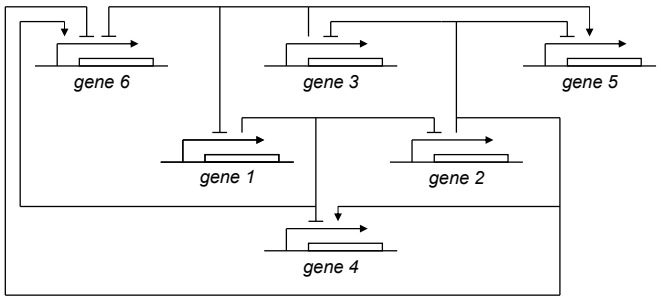

Fig. 5. Artificial regulatory network (repressilator loop plus controlled genes).

$$\tilde{L}_{\max,\vee}(\mathscr{D}', p_\vee) = \\ = \mathrm{Conv}\left(\bigcup_{k \in \mathcal{K}(\mathscr{D}')} \{z \in \mathbb{R}^2 : z_1 \le l(x^k_{j_1}), z_2 \le l(x^k_{j_2})\} \right) \tag{16}$$

that is represented in Fig. 4, to be compared to Fig. 3(a). We defer the reader to Appendix B for a general discussion of the robustification technique.

6. EXAMPLES AND DISCUSSION OF THE RESULTS

In order to assess the falsification capability provided by convexity-like properties, we considered the same artificial network introduced in Porreca et al. (2010) for evaluating the performance of the m-inconsistency analysis. The network, represented in Fig. 5, comprises 6 genes and several interactions. In particular, genes 1–3 represent the core oscillating part of the system and correspond to the repressilator network developed and synthesized in *Escherichia coli* by Elowitz and Leibler (2000). The remaining three genes are those of interest in our study and are regulated by the three core genes according to different logical rules. The dynamics of this part of the network is modeled as

$$\dot{x}_4 = \kappa_{0,4} + \kappa_{1,4}\sigma^-(x_1)\sigma^+(x_2) - \gamma_4 x_4, \tag{17a}$$
$$\dot{x}_5 = \kappa_{0,5} + \kappa_{1,5}[1 - \sigma^+(x_2)\sigma^-(x_3)] - \gamma_5 x_5, \tag{17b}$$
$$\dot{x}_6 = \kappa_{0,6} + \kappa_{1,6}[1 - \sigma^+(x_2)\sigma^+(x_3)]\sigma^+(x_1) - \gamma_6 x_6. \tag{17c}$$

where x_i, $i = 1, \ldots, 6$, denotes the concentration of the ith gene product and $\sigma^\pm(\cdot)$ are Hill functions. We defer the reader to the supplementary material of Porreca et al. (2010) for the details about the complete model and the parameter values. It is easy to recognize regulation functions in both S_0 (gene 4) and S_1 (genes 5 and 6).

We have tested the performance of both the m-inconsistency analysis and its combined use with c-inconsistency on the following datasets. The model was simulated for 15 time units [6], i.e. until 3 full oscillations were completed. To evaluate the sensitivity of our approach to the amount of data, we produced three datasets comprising $m = 45$, 23 and 12 equally spaced data points. In order to assess the impact of measurement errors, noisy synthesis rate and concentration data $\tilde{g}^k$ and $\tilde{x}^k$ were obtained by corrupting g^k and x^k with multiplicative noise, i.e., for $i = 1, \ldots, n$,

$$\tilde{x}^k_i = x^k_i(1 + s_e e^k_i) \ , \tag{18}$$
$$\tilde{g}^k_i = g^k_i(1 + s_\epsilon \epsilon^k_i) \ , \tag{19}$$

with e^k_i and ϵ^k_i mutually uncorrelated Gaussian random variables with zero mean and unit variance (Porreca et al., 2010). The scaling factors s_e, s_ϵ were chosen in the set $\{0.03, 0.05, 0.07\}$ in order to model noise contributions ranging from the 10% to the 20% of the noiseless values. In order to establish lower and upper bounds to the data, as assumed in Section 5.1, we used 95% confidence intervals resulting in

$$l(\tilde{x}^k_i) = \tilde{x}^k_i(1 - 2s_e) \ , \quad u(\tilde{x}^k_i) = \tilde{x}^k_i(1 + 2s_e) \ , \tag{20}$$
$$l(\tilde{g}^k_i) = \tilde{g}^k_i(1 - 2s_\epsilon) \ , \quad u(\tilde{g}^k_i) = \tilde{g}^k_i(1 + 2s_\epsilon) \ . \tag{21}$$

Since this gene network model involves Hill functions, the log-transformation discussed in Example 1 was applied to the data prior to the execution of Algorithm 1.

We are interested in comparing the falsification performance of the c-consistency analysis to the case when only m-inconsistency is used. To this purpose, let $N_{\text{c-inc}}$ be the number of c-inconsistent structures and $N_{\text{m-inc}}$ the number of m-inconsistent structures. The performance index $I_\% \ge 0$ is defined as the percentage improvement in the number of falsified structures, i.e.

$$I_\% = \frac{N_{\text{c-inc}} - N_{\text{m-inc}}}{N_{\text{m-inc}}} \cdot 100 \ . \tag{22}$$

In order to quantify the fraction of all structures that are falsified, we also introduce the selectivity index

$$S_\% = \frac{N_{\text{c-inc}}}{|S_0 \cup S_1|} \cdot 100 \ , \tag{23}$$

where the total number of structures is $|S_0 \cup S_1| = 5588$ for the considered network. Average values of the performance indices are reported in Table 1 for varying values of dataset size m and noise scaling factors s_e, s_ϵ. They were obtained from 100 Monte Carlo experiments, each characterized by different noise realizations.

The true structure was never declared inconsistent, showing the reliability of the falsification procedure. Concerning the selectivity index $S_\%$, one can notice a degradation of performance when either the noise level increases or the size of the dataset decreases. The variability of $S_\%$ among the three genes also suggests that the considered datasets do not equally support structure falsification for different genes. The analysis of index $I_\%$ highlights an interesting behavior. Excluding the less favorable condition $s_e = s_\epsilon = 0.07$ and $m = 12$, the contribution

[6] The definition of the time unit is unimportant in our study.

		s_e,s_ϵ		
m	gene	0.03	0.05	0.07
45	4	$S_\%$=47.60 $I_\%$= 5.07	$S_\%$=42.30 $I_\%$= 5.35	$S_\%$=37.06 $I_\%$= 6.47
	5	$S_\%$=41.46 $I_\%$= 6.65	$S_\%$=31.23 $I_\%$= 8.54	$S_\%$=23.84 $I_\%$=12.08
	6	$S_\%$=40.19 $I_\%$= 6.01	$S_\%$=36.36 $I_\%$= 8.30	$S_\%$=31.25 $I_\%$=10.53
23	4	$S_\%$=45.00 $I_\%$= 7.92	$S_\%$=38.57 $I_\%$= 8.73	$S_\%$=32.86 $I_\%$= 9.28
	5	$S_\%$=34.81 $I_\%$= 8.65	$S_\%$=26.39 $I_\%$=12.13	$S_\%$=19.03 $I_\%$=13.03
	6	$S_\%$=37.66 $I_\%$=10.09	$S_\%$=32.86 $I_\%$=12.97	$S_\%$=27.29 $I_\%$=14.18
12	4	$S_\%$=41.78 $I_\%$= 9.63	$S_\%$=33.37 $I_\%$=10.84	$S_\%$=25.28 $I_\%$=10.99
	5	$S_\%$=29.44 $I_\%$=11.54	$S_\%$=22.37 $I_\%$=12.76	$S_\%$=16.62 $I_\%$=12.19
	6	$S_\%$=32.82 $I_\%$=10.88	$S_\%$=27.88 $I_\%$=12.87	$S_\%$=23.44 $I_\%$=12.45

Table 1. Performance results on the example network.

of the c-inconsistency analysis increases when datasets become smaller and noisier. A more thorough analysis of the results in Table 1, taking into account the complexity of the falsified structures (i.e., the number of effective inputs of g), also reveals that the improvement is more significant (up to 40%) as the complexity increases (results not shown). This means that c-inconsistency can play a key role in situations when structures of higher complexity need to be falsified on the basis of few noisy data.

7. CONCLUSIONS

In this paper, we introduced and analyzed geometrical properties of a relevant class of gene network models. Under the assumption that measurements of gene product concentrations and synthesis rates are available, we exploited monotonicity and convexity-like properties in order to falsify a number of model structures that are inconsistent with the data. The proposed falsification techniques represent an extension of the approach presented in Porreca et al. (2010), where the concept of sign pattern was introduced to capture the monotone character of gene regulation functions.

The performance of the method was evaluated by means of Monte Carlo simulation using an oscillating synthetic network model. Results have shown a nonnegligible improvement with respect to the approach in Porreca et al. (2010), especially when a small, noisy dataset is used.

Future directions of this research include the analysis of the hierarchical properties of c-inconsistent model structures and their exploitation for reducing the computational complexity of the model invalidation algorithms.

ACKNOWLEDGEMENTS

This work was partially supported by the European Commission under the Network of Excellence HYCON2, contract number FP7-ICT-257462, and by the SystemsX.ch research consortium under the project YeastX.

REFERENCES

Boyd, S. and Vandenberghe, L. (2004). *Convex Optimization*. Cambridge University Press, Cambridge.

de Jong, H. (2002). Modeling and simulation of genetic regulatory systems: A literature review. *J. Comput. Biol.*, 9(1), 69–105.

de Jong, H., Ranquet, C., Ropers, D., Pinel, C., and Geiselmann, J. (2010). Experimental and computational validation of models of fluorescent and luminescent reporter genes in bacteria. *BMC Systems Biology*, 4(1), 55.

Elowitz, M. and Leibler, S. (2000). A synthetic oscillatory network of transcriptional regulators. *Nature*, 403(6767), 335–338.

Grefenstette, J., Kim, S., and Kauffman, S. (2006). An analysis of the class of gene regulatory functions implied by a biochemical model. *BioSystems*, 84, 81–90.

Hanoch, G. and Rothschild, M. (1972). Testing the assumptions of production theory: A nonparametric approach. *The Journal of Political Economy*, 80(2), 256–275.

Kauffman, S., Peterson, C., Samuelsson, B., and Troein, C. (2004). Genetic networks with canalyzing boolean rules are always stable. *PNAS*, 101(49), 17102–17107.

Kvasnica, M., Grieder, P., and Baotić, M. (2004). Multi-Parametric Toolbox (MPT). URL `http://control.ee.ethz.ch/~mpt/`.

Nikolajewa, S., Friedel, M., and Wilhelm, T. (2007). Boolean networks with biologically relevant rules show ordered behavior. *BioSystems*, 90, 40–47.

Plahte, E., Mestl, T., and Omholt, S. (1998). A methodological basis for description and analysis of systems with complex switch-like interactions. *J. Math. Biol.*, 36, 321–348.

Porreca, R., Cinquemani, E., Lygeros, J., and Ferrari-Trecate, G. (2010). Identification of genetic network dynamics with unate structure. *Bioinformatics*, 26(9), 1239–1245.

Sontag, E. (2008). Network reconstruction based on steady-state data. *Essays in Biochemistry*, 45, 161–176.

Szallasi, Z. and Liang, S. (1998). Modeling the normal and neoplastic cell cycle with "realistic boolean genetic networks": their application for understanding carcinogenesis and assessing therapeutic strategies. In *Proc. Pacific Symposium on Biocomputing*, volume 3, 66–76.

Appendix A. MATHEMATICAL PROOFS

Proof of Proposition 2: If p is the sign pattern of g then $z \in \square(x^k, p)$ implies $g(z) \geq g(x^k)$. Then $z \in \bigcup_{k\in\mathcal{K}(\mathscr{D}')} \square(x^k, p)$ implies $g(z) \geq \min_{k\in\mathcal{K}(\mathscr{D}')} g^k$, i.e. $M(\mathscr{D}', p) \subseteq T_{\mu(\mathscr{D}')}(g)$.

Proof of Proposition 3: If g is log-convex, for every $\alpha \in [0,1]$ and every $x, y \in D$, one gets $g\big(\alpha x + (1-\alpha)y\big) \leq g(x)^\alpha g(y)^{1-\alpha} \leq \min\{g(x), g(y)\}^\alpha \cdot \min\{g(x), g(y)\}^{1-\alpha} = \min\{g(x), g(y)\}$. Hence g is quasi-convex. The fact that log-concave functions are also quasi-concave is proven similarly.

Proof of Proposition 4: (a) Let p be the sign pattern of (9). Up to a suitable renormalization for the zero entries of p, (9) can be written as

$$f(x) = \prod_{j=1}^{n} \left(1 + e^{-p_j d_j (x_j - \eta_j)}\right)^{-1}.$$

By double differentiation, the Hessian of $-\log f(x)$ is found to be

$$\operatorname{diag}\left\{ \frac{p_1^2 d_1^2 e^{-p_1 d_1 (x_1-\eta_1)}}{\left[1+e^{-p_1 d_1 (x_1-\eta_1)}\right]^2}, \cdots, \frac{p_n^2 d_n^2 e^{-p_n d_n (x_n-\eta_n)}}{\left[1+e^{-p_n d_n (x_n-\eta_n)}\right]^2} \right\},$$

which is a positive semidefinite matrix for all x and all parameter values. Hence $-\log b(x)$ is convex, i.e. $b(x)$ is log-concave. Quasi-concavity follows from Proposition 3. The same holds if the Hessian is computed w.r.t. any subvector of x. (b) The log-concavity and quasi-concavity of $b_\wedge(x)$ w.r.t. to $(x_{j_3}, \dots x_{j_\ell})$ is proven as above. Similarly, $\sigma^{\pm}(x_{j_1})\sigma^{\pm}(x_{j_2})$ is quasi-concave w.r.t. x_{j_1}, x_{j_2}, hence $-\sigma^{\pm}(x_{j_1})\sigma^{\pm}(x_{j_2})$ is quasi-convex and so is $b_\vee(x)$.

Proof of Proposition 5: Since $S_0(p) \subseteq U(p)$, from Proposition 2 it follows that $M(\mathscr{D}', p) \subseteq T_{\mu(\mathscr{D}')}(g)$. From Proposition 4(a), it also follows that $g(x)$ is quasi-concave i.e. for any $\varepsilon \geq 0$, $T_\varepsilon(g)$ is a convex set. Hence, $M(\mathscr{D}', p) \subseteq T_{\mu(\mathscr{D}')}(g)$ implies $\operatorname{Conv}\big(M(\mathscr{D}', p)\big) \subseteq T_{\mu(\mathscr{D}')}(g)$.

Proof of Lemma 6: For every k it holds that $a_k b_k \leq a^* b_k$, where $a^* = \max_k a_k$. Then $\min_k(a_k b_k) \leq \min_k(a^* b_k) = a^* \min_k b_k$, which proves the leftmost inequality. Similarly, for every k it holds that $a_k b_k \geq a_k b^*$, where $b^* = \min_k b_k$. Then $\max_k(a_k b_k) \geq \max_k(a_k b^*) = (\max_k a_k) b^*$, which proves the rightmost inequality.

Proof of Proposition 7: We first prove the last inclusion in a way similar to Proposition 5. By the monotonicity properties of $b_\wedge$, for any $x_\wedge \in \mathbb{R}^{\ell-2}$, $\square^+_\wedge(x_\wedge, p_\wedge) \subseteq T_{b_\wedge(x_\wedge)}(b_\wedge)$. Hence if $z \in \bigcup_{k\in\mathcal{K}(\mathscr{D}')} \square^+_\wedge(x^k_\wedge, p_\wedge)$ then $b_\wedge(z) \geq \min\{b_\wedge(x^k_\wedge) : \ k \in \mathcal{K}(\mathscr{D}')\}$, i.e. the union is contained in $T_{\mu_\wedge(\mathscr{D}')}(b_\wedge)$. Since $b_\wedge$ is quasi-concave, i.e. set $T_\varepsilon(b_\wedge)$ is convex for any ε, the convex closure of the union must also be contained in $T_{\mu_\wedge(\mathscr{D}')}(b_\wedge)$. The first inclusion is proven similarly by exploiting the quasi-convexity of $b_\vee$. For the second inclusion, it suffices to note that, in light of the monotonicity of $b_\vee$, $\square^+(x_\vee, p_\vee) \subseteq T_{b_\vee(x_\vee)}(b_\vee)$ for any $x_\vee \in \mathbb{R}^2$. Hence, all elements z of $\bigcap_{k\in\mathcal{K}(\mathscr{D}')} \square^+(x^k_\vee, p_\vee)$ are such that $b_\vee(z) \geq \max\{b_\vee(x^k_\vee) : \ k \in \mathcal{K}(\mathscr{D}')\}$, i.e. the intersection is contained in $T_{\mathscr{M}_\vee(\mathscr{D}')}(b_\vee)$. The third inclusion is proven similarly.

Proof of Proposition 8: For the first implication, from Proposition 7, conditions $x^*_\vee \in L_{\max,\vee}(\mathscr{D}', p_\vee)$ and $x^*_\wedge \in L_{\min,\wedge}(\mathscr{D}', p_\wedge)$ imply $b_\vee(x^*_\vee) \leq \mathscr{M}_\vee(\mathscr{D}')$ and $b_\wedge(x^*_\wedge) \leq \mu_\wedge(\mathscr{D}')$, respectively. Then, using Lemma 6,

$$b(x^*) = b_\vee(x^*_\vee) \cdot b_\wedge(x^*_\wedge) \leq \mathscr{M}_\vee(\mathscr{D}') \cdot \mu_\wedge(\mathscr{D}') \leq \max_{k\in k(\mathscr{D}')} b_\vee(x^k_\vee) b_\wedge(x^k_\wedge) = \max_{k\in k(\mathscr{D}')} b(x^k).$$

Finally, using the relations $g^* = g(x^*)$ and $g^k = g(x^k)$,

$$g^* = \kappa_0 + \kappa_1 b(x^*) \leq \kappa_0 + \kappa_1 \max_{k\in k(\mathscr{D}')} b(x^k) = \max_{k\in k(\mathscr{D}')} \kappa_0 + \kappa_1 b(x^k) = \max_{k\in k(\mathscr{D}')} g(x^k) = \mathscr{M}(\mathscr{D}').$$

The second implication is proven similarly.

Appendix B. ROBUSTIFICATION UNDER BOX UNCERTAINTY

Assume that, for all $k = 1, \dots, m$ and $j = 1, \dots, n$, we are given lower and upper bounds $l(x^k_j), l(g^k)$ and $u(x^k_j), u(g^k)$. Then it is possible to define worst-case scenarios for all falsification conditions as follows. For what concerns g_i, conditions $g^* < \mu(\mathscr{D}')$ and $g^* > \mathscr{M}(\mathscr{D}')$ are easily robustified as

$$u(g^*) < \min_{k\in\mathcal{K}(\mathscr{D}')} l(g^k)$$

and

$$l(g^*) > \max_{k\in\mathcal{K}(\mathscr{D}')} u(g^k),$$

respectively. Conditions on x all involve sets computed as combinations (union, intersection, convex hull) of cones. Robustification is achieved in this case by considering inner approximations of such sets. With reference to the notation in Section 4.2, this is obtained by using the following worst-case inner approximation $\widetilde{\square}^{\pm}(z, p)$ of any cone $\square^{\pm}(z, p)$:

$$\widetilde{\square}^+(z,p) = \{z' \in \mathbb{R}^d : \ z'_j \geq u(z_j), \ \forall j \text{ such that } p_j = 1, \ z'_j \leq l(z_j), \ \forall j \text{ such that } p_j = -1\} \ , \quad \text{(B.1a)}$$

$$\widetilde{\square}^-(z,p) = \{z' \in \mathbb{R}^d : \ z'_j \leq l(z_j), \ \forall j \text{ such that } p_j = 1, \ z'_j \geq u(z_j), \ \forall j \text{ such that } p_j = -1\} \ . \quad \text{(B.1b)}$$

Moreover, the uncertainty of point x^* is also taken into account by considering the point $\tilde{x}^*$ instead, with

$$\tilde{x}^*_j = \begin{cases} l(x^*_j), & j \text{ such that } p_j = 1, \\ u(x^*_j), & j \text{ such that } p_j = -1, \end{cases}$$

or

$$\tilde{x}^*_j = \begin{cases} u(x^*_j), & j \text{ such that } p_j = 1, \\ l(x^*_j), & j \text{ such that } p_j = -1, \end{cases}$$

for conditions involving $\square^+$ or $\square^-$ cones, respectively.